

BISTABILITY AND BORDER-COLLISION BIFURCATIONS FOR A FAMILY OF UNIMODAL PIECEWISE SMOOTH MAPS

IRYNA SUSHKO

Institute of Mathematics
National Academy of Sciences of Ukraine
3 Tereshchenkivska st.
01601 Kiev, Ukraine

ANNA AGLIARI

Faculty of Economics, Catholic University
Via Emilia Parmense, 84
49100 Piacenza, Italy

LAURA GARDINI

Faculty of Economics, University of Urbino
via Saffi 42
61029 Urbino (PU), Italy

ABSTRACT. This article deals with a two-parameter family of piecewise smooth unimodal maps with one break point. Using superstable cycles and their symbolic representation we describe the structure of the periodicity regions of the 2D bifurcation diagram. Particular attention is paid to the bistability regions corresponding to two coexisting attractors, and to the border-collision bifurcations.

1. Introduction. The theory of one-dimensional (1D henceforth) *smooth* discrete dynamical systems is well developed since many years. Regarding to the deterministic approach we refer to [3], [8], [9], [20], [25] (to cite a few). Particularly developed is the bifurcation theory of smooth *unimodal* maps, based on the study of the logistic map $g : x \mapsto g(x) = ax(1-x)$ as the parameter a varies in the interval [3, 4].

However, in the investigation of the dynamic properties of applied models the corresponding functions are often only *piecewise smooth* (or piecewise linear). Examples of the relevant models coming from economics can be found in [6], [7], [13],

2000 *Mathematics Subject Classification.* Primary: 37E05, 37G35; Secondary: 37N30.

Key words and phrases. Unimodal piecewise smooth map, bifurcation diagram, border-collision bifurcation, bistability.

This work has been performed within the activity of the national research project “Nonlinear models in economics and finance: complex dynamics, disequilibrium, strategic interactions”, MIUR, Italy. I.Sushko thanks the Landau Network/Cariplo Foundation, and a Marie Curie International Fellowship (within the 6th European Community Framework Programme) which supported the revised version.

[23], [24]. See also [27] with examples and references related to piecewise smooth dynamical systems coming from biology, engineering and other sciences.

The bifurcation theory of piecewise smooth dynamical systems is less developed. For such systems we can in general distinguish between two types of bifurcations: One includes the bifurcations which occur in smooth dynamical systems (either local, associated with the eigenvalues $+1$ or -1 , or global, associated with the homoclinic bifurcation of some cycle, or to the limit set of some sequence of bifurcation values), while the other is the so-called *border-collision bifurcation* [21]. This bifurcation, specific for piecewise smooth maps, occurs when a trajectory collides with one of the break points, separating intervals in which the map changes its definition. In general, crossing such a point, there is a discontinuous change in the derivative, and this may cause an abrupt transition in the structure and stability of attracting and repelling invariant sets. The effect of the merging of a periodic point with a border point, i.e. the effect of the border-collision bifurcation, is not unique. We may have the abrupt transition from an attracting cycle to another attracting cycle of any period (which may also appear with several or infinitely many repelling cycles), or to cyclical chaotic intervals of any period.

It is now known that the study of the bifurcations associated with piecewise smooth systems started in the Russian literature with the works by Feigen (in the decade 1970-1980), however they came to the knowledge of a wide public only recently, by the translation of his main results in [4]. In this paper some analytical conditions are given related to the possible consequences of a border-collision bifurcation in n -dimensional piecewise smooth systems. In that literature the bifurcations associated with the border points are called *C-bifurcations* (see also [11]). While the term *border-collision bifurcation* was introduced by Nusse and Yorke [21], [22]. In these papers the authors examine bifurcation phenomena for 1D and 2D piecewise smooth maps and state explicitly which border-collision bifurcation does occur depending on parameters. Their approach was developed in later papers (see, for example, [1], [2]) in which the possible border-collision bifurcations are classified according to the parameters of corresponding *normal form* which is the piecewise linear approximation of the map in the neighborhood of the break point.

At the same time, a different kind of analysis of the bifurcation sequences, allowed in *piecewise linear* maps, has been performed in [16], [17] (for a unimodal map with one break point), and in [18] (for a bimodal map with two break points). It was shown that for piecewise linear maps one of the most relevant characteristics is the absence of cascade of period-doubling bifurcations of periodic orbits. The transitions are reduced to a few cascades of band merging bifurcations of cyclical chaotic intervals, while periodic orbits are organized in a *period-adding* sequence. This is mainly due to the vanishing of second and higher order derivatives causing the collision in one bifurcation point of several bifurcations which for smooth maps occur at separate bifurcation values.

Typical for piecewise smooth dynamical systems is the so-called “sausage” structure of the periodicity tongues in the parameter space, first described in [12] in the case of a piecewise linear 1D map, and then generalized for higher dimensions in [27], see also [24].

The object of the present paper is to investigate the dynamic properties of a particular two-parameter family of piecewise smooth unimodal maps with one break point. Following the economic model proposed in [5], we consider the map f defined by a piecewise smooth function $f(x)$ which consists on a linear function joined with

the logistic in a break point \bar{x} , namely,

$$f : x \mapsto f(x) = \begin{cases} f_1(x) = rx, & \text{if } 0 \leq x < \bar{x}; \\ f_2(x) = ax(1-x), & \text{if } \bar{x} \leq x \leq 1; \end{cases} \quad \bar{x} = 1 - \frac{r}{a}, \quad (1)$$

where a and r are real parameters varying in the ranges $a > 3$ and $1 < r < a$. We shall see that the complexity of the two-dimensional (2D henceforth) bifurcation diagram in the (r, a) -parameter plane is associated with local and global bifurcations due to the smooth part of the function $f(x)$, combined with the border-collision bifurcations due to the existence of the break point \bar{x} at which the function $f(x)$ changes definition.

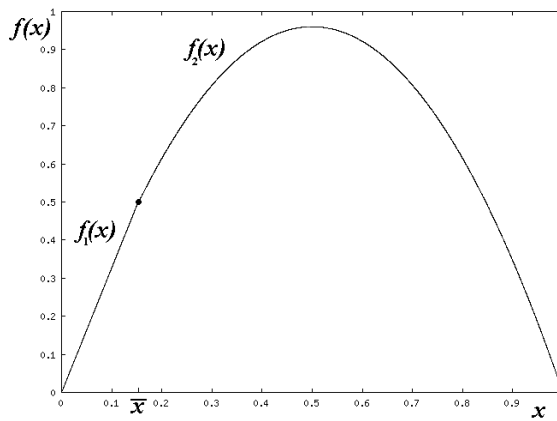


FIGURE 1. The function $f(x)$ at $r = 3.268$, $a = 3.8406$, in case of coexisting attracting 3-cycle and attracting 6-cycle.

The peculiar property of this unimodal map is the existence of infinitely many regions of bistability in the (r, a) -parameter plane, corresponding to two coexisting attractors (cycles or chaotic intervals), although the shape of the function $f(x)$ seems not suggest this peculiarity: See Fig.1 where $f(x)$ is shown in a case of coexisting attracting 3-cycle and attracting 6-cycle (this case is commented in detail in Section 4).

We recall that for smooth maps g (such as the logistic), the bifurcation scenario is related to the curvature of the function $g(x)$, and since Singer [26] relevant results are associated with the notion of *Schwarzian derivative* $Sg(x)$ ¹. It is proved (see also [8], or [3]) that for unimodal C^3 maps with one critical (turning) point and negative Schwarzian there exists at most one attractor which attracts the critical point, plus possibly a stable fixed point attracting a boundary point of I . This result holds also for unimodal C^1 maps with piecewise monotone first derivative and negative Schwarzian for each monotone branch (see [3] with an example of such a map with two coexisting attractors). An analogous result is proved for unimodal C^1 maps consisting of pieces of linear-fractional functions which have zero Schwarzian [25] (it can be shown that unimodal maps with positive or zero Schwarzian cannot be differentiable at the extremum point). Other examples of unimodal maps with

¹ $Sg(x) = \frac{g'''(x)}{g'(x)} - \frac{3}{2}(\frac{g''(x)}{g'(x)})^2$

two coexisting attractors are given in [26], [19]. The Schwarzian derivative of the function $f(x)$ given in (1) is $Sf(x) = 0$ for $x < \bar{x}$ and $Sf(x) < 0$ for $x > \bar{x}$. It can be shown that also the map f can have at most two attractors: In case of bistability the critical point (the local maximum) is attracted by one attractor while the break point is attracted by the other one (an example, studied in details in Section 4, is shown in Fig.6).

The next sections are devoted to the investigation of the structure of the 2D bifurcation diagram of the map f in the (r, a) -parameter plane. The plan of the paper is as follows. In Section 2 we first present some simple properties of the map f . Then we recall briefly what is known for the logistic map about its attractors and bifurcation structure of the interval $[3, 4]$, in which the parameter a varies, and give the conditions under which these results are applied for the map f . In Section 3, using the symbolic representation of the superstable n -cycle of the map f , we describe a sequence of collisions with \bar{x} (i.e., the sequence of BC), followed by a border-collision bifurcation (BCB), related to this cycle under specified parameter variation. Bistability regions in the (r, a) -parameter plane are described in Section 4. We show that the boundaries of the bistability regions in the (r, a) -parameter plane are formed by fold, period-doubling and border-collision bifurcation curves.

2. “Logistic” Part of the Bifurcation Plane. Let us derive some simple properties and propositions for the map f defined in (1). In the considerations given below we assume $(r, a) \in R = \{(r, a) : a > 3, 1 < r < a\}$.

Property 1. *The map (1) has two fixed points $x = 0$ and $x^* = 1 - 1/a$, both unstable for $(r, a) \in R$.*

The notion of *critical (turning) point* is usually associated with a local extremum of the function: In the smooth case $f'(x) = 0$ at such a point, while in the piecewise smooth case the local extremum can be in a break point in which the derivative is not defined. For the map (1) we have the two possibilities, as stated in the following property:

Property 2. *The local extremum (maximum) of the function (1) is at the break point \bar{x} for $r \leq a/2$, and at the critical point $x_c = 1/2$ for $r \geq a/2$.*

Using the above property we can easily get the condition for the interval $I = [0, 1]$ to be trapping for the map f (i.e., $f(I) \subseteq I$):

Proposition 1. *If $(r, a) \in D \subset R$, where*

$$D = \{(r, a) : r < 2, a \leq r^2/(r - 1)\} \cup \{(r, a) : r \geq 2, a \leq 4\},$$

then the interval I is trapping for f .

In the (r, a) -parameter plane the curves $a = r^2/(r - 1)$ (for $r < 2$) and $a = 4$ (for $r \geq 2$), at which the interval I is invariant (i.e., $f(I) = I$), correspond to the so-called *boundary crisis* bifurcation (homoclinic bifurcation of the origin). If the (r, a) -parameter point is taken above these curves then almost all the trajectories of the map f go to infinity, and the surviving set is a Cantor set $\Lambda \subset I$ which is invariant, also called a *chaotic repeller*.

We shall investigate the parameter range in which the interval I is trapping, i.e., we take the parameter values $(r, a) \in D$ and, thus, $f : [0, 1] \rightarrow [0, 1]$.

First of all we recall that a compact invariant set A is said *attracting set* of a 1D map f if a neighborhood $U(A)$ exists such that for any $x \in U(A)$, $f^n(x) \in U(A)$ for

any n , and $f^n(x) \rightarrow A$ as $n \rightarrow \infty$. An *attractor* \mathcal{A} is an attracting set with a dense trajectory. The attractor of a 1D map can be either an attracting k -cycle (i.e., a periodic orbit of period k) or an attracting k -cyclic chaotic interval (i.e., a cycle of chaotic intervals of period k).

To proceed it is worth to recall briefly what is known for the logistic map $g : x \mapsto g(x) = ax(1 - x)$ about the bifurcation structure of the interval $[3, 4]$ in which the parameter a varies. It is known that

- 1) the set $\mathcal{P} = \{a : \mathcal{A} \text{ is a periodic orbit}\}$ is dense and consists of countably many nontrivial intervals [10]. Moving inside one connected component of \mathcal{P} we see the period-doubling scenario;
 - 2) the set $\mathcal{I} = \{a : \mathcal{A} \text{ is a cycle of chaotic intervals}\}$ is a completely disconnected set of positive Lebesgue measure [14];
 - 3) the complementary set $\mathcal{C} = [3, 4] \setminus \mathcal{P} \setminus \mathcal{I}$ is a completely disconnected set of zero Lebesgue measure [15];
- (see also [8] for the details and more references).

These results refer to the well-known 1D bifurcation diagram for the logistic map with countably many windows of periodicity (the set \mathcal{P}), limit points for period-doubling cascades (belonging to the set \mathcal{C} together with limit points for other bifurcation values) and values of a corresponding to cycles of chaotic intervals (the set \mathcal{I}). Each new periodicity window is originated by a *fold (or tangent) bifurcation* followed by a cascade of *period-doubling bifurcations* up to the Feigenbaum accumulation point. From the opposite side this point is the accumulation point for other cascades of bifurcations, among which we indicate homoclinic bifurcations giving rise to band-merging of chaotic intervals.

Recall now that an interval $J \subset I$ is said to be *absorbing* for a 1D continuous map f if a) $f(J) \subseteq J$; b) a neighborhood $U(J)$ exists such that for any $x \in U(J)$ a finite integer m exists such that $f^n(x) \in J$ for any $n > m$; c) the boundary of J is made up by images of a critical point. In other words, the absorbing interval J is such that after a finite number of iterations the forward images of a point $x \in U(J)$ enter J and cannot escape from it. So, an attractor of the map f must belong to its absorbing interval.

The absorbing interval J of the logistic map is bounded by two images of the critical point $x_c = 1/2$, namely, $J = [g^2(x_c), g(x_c)]$.

Regarding the map f given in (1) the results known for the logistic map are applied (for some fixed r) if the absorbing interval J of the map f is included in the interval where this map is defined by the logistic function only, i.e., if $J \subseteq [\bar{x}, 1]$, that is if $f^2(x_c) \geq \bar{x}$. The last inequality is satisfied under the condition stated in the following

Proposition 2. *If*

$$r \geq r_l(a) \stackrel{def}{=} a^4/16 - a^3/4 + a \tag{2}$$

then the absorbing interval $J = [f^2(x_c), f(x_c)]$ of the map (1) is included in $[\bar{x}, 1]$.

Thus, a parameter region $D_l \subset D$, for which (2) is satisfied (see Fig.2), has the “logistic” bifurcation structure in the following sense: In order to comment a 1D bifurcation diagram, if we fix a parameter point $(r, a) = (r^*, a^*) \in D_l$ and move it increasing a , up to the point $(r^*, a^{**}) \in r_l(a)$, then we get the 1D bifurcation diagram of the logistic map for $a \in [a^*, a^{**}]$.

Answer to the questions of how the different attracting cycles of the logistic map are ordered on the parameter a , and how many attracting cycles of the same period n exist, can be get from the theory of symbolic dynamics (see [19], [12]), or from the description of the “box-within-a-box” bifurcation structure (see [20]). Now we recall only that the logistic map has k attracting cycles of the same period n for different values of a , where the corresponding values of the pair (k, n) are $(1, 2)$, $(1, 3)$, $(2, 4)$, $(3, 5)$, $(5, 6)$, $(9, 7)$, $(16, 8), \dots$. These k different attracting n -cycles are ordered on a according to the order of their symbolic sequences.

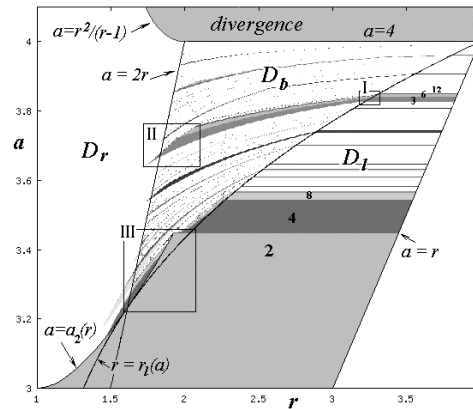


FIGURE 2. Two-dimensional bifurcation diagram of the map f in the (r, a) -parameter plane. The regions P_n corresponding to attracting cycles of period n , $n \leq 24$, are shown by different gray tonalities for different n .

Let P_n denote a region in the (r, a) -parameter plane such that for $(r, a) \in P_n$ the map (1) has an attracting cycle of period n (note that we use the same notation P_n for different regions of the same periodicity, that is, there exist k different regions P_n). Fig.2 presents a 2D bifurcation diagram of the map f in the (r, a) -parameter plane where the regions P_n are shown by different gray tonalities for different n , $n \leq 24$. Obviously, the lower boundary of the periodicity region $P_n \cap D_l$ corresponds to either a fold bifurcation (giving rise to a new periodicity “box”), or a period-doubling bifurcation, while its upper boundary is a period-doubling bifurcation curve.

3. Superstable Cycles and “Skeleton” of the Bifurcation Plane. Denote by D_b a region in the (r, a) -parameter plane such that $x_c \geq \bar{x}$ and $\bar{x} \in J$, that is

$$D_b = \{(r, a) : a/2 \leq r \leq r_l(a), 3 < a < 4\},$$

where $r_l(a)$ is given in (2) (see Fig.2). In this section we investigate the structure of the periodicity regions $P_n \cap D_b$.

Let $\gamma_{i,j}$ denote an attracting cycle of period $n = i + j$, $i \geq 0$, $j > 0$, of the map f , such that i points of the cycle belong to the segment $[0, \bar{x}]$ (where the map f is defined by the linear function $f_1(x)$) and j points belong to $[\bar{x}, 1]$ (where f is defined by the logistic function $f_2(x)$).

If a point of the n -cycle of the map f collides with the break point under the change in the parameters, we say that a *border-collision* (BC henceforth) occurs for this cycle. It is in general accompanied with discontinuous change in the derivative of $f(x)$ at this point. Moreover, if after such a collision the *orbit index* [22] of the border-crossing cycle changes, i.e., there is a qualitative change in the dynamics of the map, we say that a *border-collision bifurcation* (BCB henceforth) occurs for the cycle. (Recall that a cycle has orbit index 1 if its eigenvalue $|\lambda| < 1$, -1 if $\lambda > 1$ and 0 if $\lambda < -1$).

The considerations given in this section are based on the study of *superstable cycles* $\gamma_{i,j}$ (i.e., such that x_c is a point of the cycle). We use the superstable cycles because the (r, a) -parameter values corresponding to such cycles form the “skeleton” of the 2D bifurcation diagram, in the same way as the values of a corresponding to the superstable n -cycles of the logistic map characterize periodic windows of the 1D bifurcation diagram. And as for the logistic map, also for the map (1) the description of the bifurcation structure, based on the superstable cycles, can be extended by continuity to some neighborhood corresponding to other attracting cycles inside the periodicity region. An attracting (not superstable) cycle is denoted $\tilde{\gamma}_{i,j}$.

As a starting point it is reasonable to consider the cycle $\gamma_{0,n}$, $n > 2$, existing for $(r, a) \in (P_n \cap D_l)$, that is, the superstable n -cycle of the logistic map. Then we decrease r until the left-hand (minimal) point of the cycle collides with the break point \bar{x} . In such a way the first BC for the cycle $\gamma_{0,n}$ occurs resulting in the cycle $\gamma_{1,n-1}$ which is obviously also superstable. We write $\gamma_{0,n} \Rightarrow \gamma_{1,n-1}$ to denote this collision. Then we continue to decrease the parameter values in such a way that the (r, a) -parameter point follows the superstable cycle $\gamma_{1,n-1}$, until one more periodic point undergoes the BC: $\gamma_{1,n-1} \Rightarrow \gamma_{2,n-2}$. And so on, up to the BC which occurs for the critical point x_c . Obviously, this is the last BC for the superstable n -cycle, occurring when $x_c = \bar{x}$, which holds for $a = 2r$ (the left boundary of the considered region D_b).

To see that the last border-collision leads to a bifurcation of the superstable n -cycle, we can apply to the map f at $a = 2r$ the classification criterion stated in [1]. In this paper it is shown that to classify the BCB of the border-crossing fixed point of a 1D piecewise smooth map, one has to analyze the parameters of the normal form, which is the piecewise linear approximation of the map in the neighborhood of the break point. For the superstable n -cycle of the map f one of these parameters is obviously zero, thus, depending on the second parameter, there can be two results of the bifurcation: 1) The superstable n -cycle loses its stability while an attracting cycle of double period $2n$ appears (an analog of the period-doubling bifurcation for smooth maps); 2) A *border-collision pair bifurcation* occurs when a point of the superstable n -cycle and a point of the repelling n -cycle collide with the break point, and these cycles disappear (an analog of the fold bifurcation).

It is obvious that under the parameter variation described above, only periodic points which are on the left of x_c can collide with \bar{x} before x_c itself collides with \bar{x} . Here we can make use of the *symbolic representation*² of the cycle $\gamma_{0,n}$ and state that the total number of admissible BC for $\gamma_{0,n}$ is equal to the number b of the

²We refer to the symbolic representation of the superstable n -cycles $\{x_i\}_{i=1}^n$ (see [19]), which starts from the first iterate of the critical point x_c , i.e., from $x_1 = f(x_c)$. We write R if $x_i > x_c$, or L if $x_i < x_c$, or C if $x_i = x_c$, for $i = 1, \dots, n$.

symbols L in the symbolic sequence of $\gamma_{0,n}$, plus the BCB occurring for the critical point x_c . Before giving the corresponding proposition let us present some examples.

Consider the periodicity regions P_3, P_6, P_{12}, \dots , (related to the period-doubling cascade of the attracting 3-cycle) included in the so-called “3-box”. Fig.3 presents the enlarged window I of the bifurcation diagram shown in Fig.2. In this figure border-collision, period-doubling and fold bifurcation curves are shown by thin, thick and dashed lines, respectively. The white curves correspond to the superstable cycles.

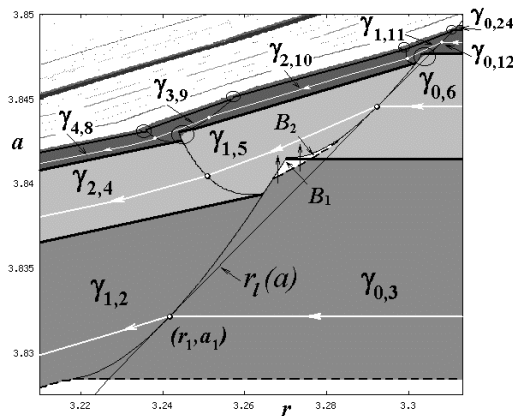


FIGURE 3. The enlarged window I of the bifurcation diagram shown in Fig.2.

Let the (r, a) -parameter point move from the right to the left inside P_3 following the superstable 3-cycle. The curve in the (r, a) -plane corresponding to the superstable cycle $\gamma_{0,3}$ satisfies

$$f_2^3(x_c) = x_c, \tag{3}$$

from where we get $a = a_1 \approx 3.8319$, while the curve of $\gamma_{1,2}$ satisfies

$$f_1 \circ f_2^2(x_c) = x_c. \tag{4}$$

The BC $\gamma_{0,3} \Rightarrow \gamma_{1,2}$ occurs at $(r_1, a_1) \approx (3.2408, 3.8319)$ satisfying both the conditions (3) and (4).

To see the left-hand part of the “3-box” we show in Fig.4 the enlarged window II of Fig.2. The BCB of the superstable 3-cycle occurs for x_c at $a = 2r$. Using this equality and the condition (4) we get the BCB parameter values $(r, a) = (r_2, a_2) \approx (1.8393, 3.6786)$. The result of this bifurcation is a repelling cycle $\gamma'_{2,1}$ of period 3 and an attracting cycle $\tilde{\gamma}_{3,3}$ of period 6.

Similarly, moving the (r, a) -parameter point from the right to the left inside P_6 , following the superstable 6-cycle, one can observe a BC sequence of this cycle (see Figs 3, 4). The symbolic representation of the considered cycle $\gamma_{0,6}$ is $\Sigma = (RL^2RLC)^\infty$, with three symbols L , thus, this cycle can undergo three BC, namely, $\gamma_{0,6} \Rightarrow \gamma_{1,5} \Rightarrow \gamma_{2,4} \Rightarrow \gamma_{3,3}$, and the BCB occurring for x_c at $a = 2r$.

The superstable cycle $\gamma_{0,6}$ satisfies

$$f_2^6(x_c) = x_c. \tag{5}$$

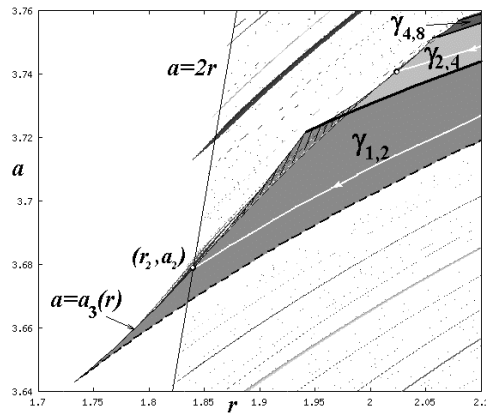


FIGURE 4. The enlarged window II of Fig.2.

To write down the conditions corresponding to the cycles $\gamma_{1,5}$, $\gamma_{2,4}$ and $\gamma_{3,3}$ we need to know 1) the location of the periodic points on the x -axis to see for which point the next BC occurs; 2) the corresponding composition of the functions $f_1(x)$ and $f_2(x)$ in the condition $f^6(x_c) = x_c$.

This information can be get using again the symbolic sequence Σ of the cycle $\gamma_{0,6}$. First we write down the sequences corresponding to each point of the cycle by shifting one symbol, then use the *ordering rule*³ for these symbolic sequences, which gives also the order of coordinates of the periodic points (see Table 1).

k	Σ_k	order
1	$RLRLC$	6
2	$LLRLCR$	1
3	$LRLCRL$	3
4	$RLCRL$	5
5	$LCRLLR$	2
6	$CRLLRL$	4

TABLE 1. The shift sequences of $(RL^2RLC)^\infty$ and their order.

Now let us introduce the symbolic representation Σ' of the superstable cycle $\gamma_{i,j} = \{x_k\}_{k=1}^n, i \geq 1, j = n - i$. We start from the first iterate of the critical point x_c , i.e., $x_1 = f(x_c)$, and write the symbol

- L_1 if $x_k < \bar{x}$;
- L_2 if $\bar{x} \leq x_k < x_c$;
- C if $x_k = x_c$ and

³Recall that the ordering rule says, that given to symbolic sequences $\Sigma_1 = \Sigma \mu \dots$ and $\Sigma_2 = \Sigma \nu \dots$ with common string Σ and next symbol $\mu \neq \nu$, the order of μ and ν (in the sence of the natural order $L < C < R$) is the order of Σ_1 and Σ_2 if Σ is even, and the order is opposite if Σ is odd. Recall also that Σ is even (odd) if the number of R in Σ is even (odd) (see [12]).

R if $x_k > x_c$,
 for $k = 1, \dots, n$. Here L_1 denotes that the function $f_1(x)$ is to be applied while the symbols L_2, R and C are related to the function $f_2(x)$.

From Table 1 we see that the *first* (ordered on coordinates) periodic point has the symbolic sequence $\sum_2 = LLRLCR$. Thus, the first BC $\gamma_{0,6} \Rightarrow \gamma_{1,5}$ (under the parameter variation described above) occurs for this point. After the collision this point is on the left of the break point and, thus, the first symbol L is related to the function $f_1(x)$. So, we can write down the symbolic sequence of the resulting cycle $\gamma_{1,5}$, which is $\sum_2' = L_1L_2RL_2CR$. Using \sum_2' we get the condition which has to be fulfilled for the cycle $\gamma_{1,5}$:

$$f_2^3 \circ f_1 \circ f_2^2(x_c) = x_c. \tag{6}$$

The BC $\gamma_{0,6} \Rightarrow \gamma_{1,5}$ occurs when both the conditions (5) and (6) hold.

Similarly, from the Table 1 we can see that the *second* (ordered on coordinates) periodic point has the symbolic sequence $\sum_5 = LCRLLR$. Thus, the second BC $\gamma_{1,5} \Rightarrow \gamma_{2,4}$ occurs for this point, after which we have two periodic points on the left of the break point and, thus, two symbols L are related to the function $f_1(x)$. So, the symbolic sequence of the resulting cycle $\gamma_{2,4}$ is $\sum_5' = L_1CRL_1L_2R$, using which we get the corresponding condition

$$f_1 \circ f_2^2 \circ f_1 \circ f_2^2(x_c) = x_c. \tag{7}$$

Thus, the BC $\gamma_{1,5} \Rightarrow \gamma_{2,4}$ occurs when the conditions (6) and (7) are satisfied.

The *third* (ordered on coordinates) periodic point (see Table 1) has the symbolic sequence $\sum_3 = LRLCRL$. Thus, the third BC $\gamma_{2,4} \Rightarrow \gamma_{3,3}$ occurs for this point, so that after the collision three periodic points are on the left of the break point and, thus, three symbols L are related to the function $f_1(x)$. So, the symbolic sequence of the resulting cycle $\gamma_{3,3}$ is $\sum_3' = L_1RL_1CRL_1$, and the corresponding condition which has to be satisfied is

$$f_1 \circ f_2 \circ f_1^2 \circ f_2^2(x_c) = x_c. \tag{8}$$

The BC $\gamma_{2,4} \Rightarrow \gamma_{3,3}$ occurs when the conditions (7) and (8) hold.

Finally, the BCB occurs for x_c when the conditions $a = 2r$ and (8) hold. We have numerically verified that, besides the critical point, one more point of $\gamma_{3,3}$ collides with the break point, as well as a point of the repelling 3-cycle $\gamma_{2,1}'$, and the result of this BCB is an attracting 3-cycle $\tilde{\gamma}_{1,2}$ (an analog of the period-halving bifurcation for the smooth maps).

Using the above procedure we can describe the BC sequence for the superstable cycle of any period. The considerations can be summarized in the following

Proposition 3. *If the (r, a) -parameter point moves continuously from the right to the left inside P_n , starting from a point $(r, a) \in (P_n \cap D_1)$, following the superstable n -cycle, then this cycle undergoes b border-collisions*

$$\gamma_{0,n} \Rightarrow \gamma_{1,n-1} \Rightarrow \dots \Rightarrow \gamma_{b,n-b},$$

and the border-collision bifurcation occurs at $a = 2r$ when the critical point x_c collides with \bar{x} . Here b is equal to the number of symbols L in the symbolic representation of $\gamma_{0,n}$.

Let us give an example. It is known for the logistic map, that the symbolic sequence of the last (ordered on a) superstable n -cycle is $(RL^{n-2}C)^\infty$, i.e., $b = n - 2$, thus, under the parameter variation described above, such a cycle undergoes $n - 2$

BC $\gamma_{0,n} \Rightarrow \gamma_{1,n-1} \Rightarrow \dots \Rightarrow \gamma_{n-2,2}$, plus the BCB occurring for x_c . Let the map f have an *attracting* cycle $\tilde{\gamma}_{n-2,2}$ existing for the parameter values taken from some neighborhood of those corresponding to the superstable cycle $\gamma_{n-2,2}$. Obviously, the cycle $\tilde{\gamma}_{n-2,2}$ has the symbolic representation $(RL_1^{n-2}R)^\infty$ or $(RL_1^{n-2}L_2)^\infty$. The BCB occurs for such a cycle if the condition $f_1^{n-2} \circ f_2^2(\bar{x}) = \bar{x}$ is satisfied, from which we get the following BCB curve:

$$a = a_n(r) \stackrel{def}{=} \frac{1}{r^{n-1}} \sum_{i=0}^n r^i.$$

Thus, for instance, the BCB curve of the attracting cycle $\tilde{\gamma}_{0,2}$ is

$$a_2(r) = \frac{1 + r + r^2}{r}, \tag{9}$$

so that the boundaries of the region P_2 are the curves $a = 3$ (corresponding to the period-doubling bifurcation of the fixed point x^*), $a = 1 + \sqrt{6}$ (period-doubling bifurcation of $\gamma_{0,2}$), $a = a_2(r)$ (the BCB of $\gamma_{0,2}$) and $a = r$ (see Fig.2). One more example is the curve of the BCB of $\tilde{\gamma}_{1,2}$:

$$a_3(r) = \frac{1 + r + r^2 + r^3}{r^2} \tag{10}$$

(see Fig.4). Obviously, the BCB of the superstable n -cycle with symbolic sequence $(RL^{n-2}C)^\infty$ occurs at the (r, a) -parameter point which is the intersection of two curves: $a = a_n(r)$ and $a = 2r$.

To end this section we emphasize that any periodicity region P_n , with its core corresponding to the superstable n -cycles, has continuation through the whole region D_b and crosses its left boundary $a = 2r$. The boundaries of $P_n \cap D_b$ are formed by curves corresponding to fold, period-doubling and border-collision bifurcations. Moreover, there are infinitely many regions of bistability which we discuss in the next section.

4. Bistability Regions. We recall that under the condition (2) the break point \bar{x} does not belong to the absorbing interval J but maps into it after a finite number of iterations and is attracted to the unique attractor \mathcal{A} of the map f_2 . We can say that in this case \bar{x} plays no role for the dynamics of the map f . While if $\bar{x} \in J$, this break point becomes an additional separator inside J so that there can exist two disjoint sets of absorbing intervals (related to the images of \bar{x} and x_c , respectively) which give rise to the existence of two different attractors, i.e., bistability.

In order to see how the images of both the critical point x_c and the break point \bar{x} can be involved in the construction of an absorbing set we first recall that set $\mathbf{J}_k = \{J_1, J_2, \dots, J_k\}$ of disjoint intervals is called *cyclic absorbing interval of period k* if

- a) each $J_i, i = 1, \dots, k$, is bounded by images of the critical point;
- b) $f(J_i) = J_{i+1}, i = 1, \dots, k - 1, f(J_k) \subseteq J_1$;
- c) each $J_i, i = 1, \dots, k$, is an absorbing interval for the map f^k .

For the map (1) besides the above set it is possible to have an analogous cyclic absorbing interval $\mathbf{G}_m = \{G_1, G_2, \dots, G_m\}$, where each $G_i, i = 1, \dots, m$, is bounded by the images of the break point \bar{x} . It may happen, as we show below, that for some parameter values $J_k \cap G_m = \emptyset$. In this case the map (1) has two different attractors \mathcal{A}_1 and \mathcal{A}_2 , one of period k and another of period m . The sets J_k and G_m are strictly included in the basins of attraction of \mathcal{A}_1 and \mathcal{A}_2 , respectively.

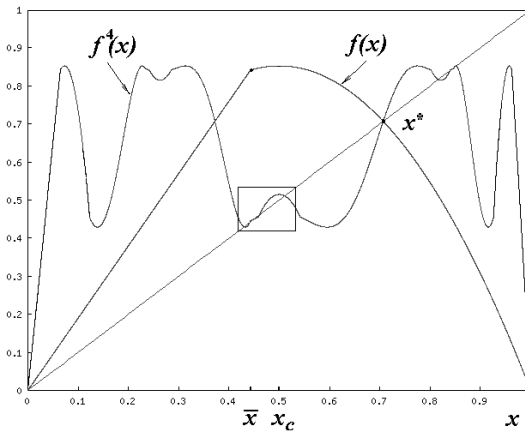


FIGURE 5. The functions $f(x)$ and $f^4(x)$ at $a = 3.41$, $r = 1.9$.

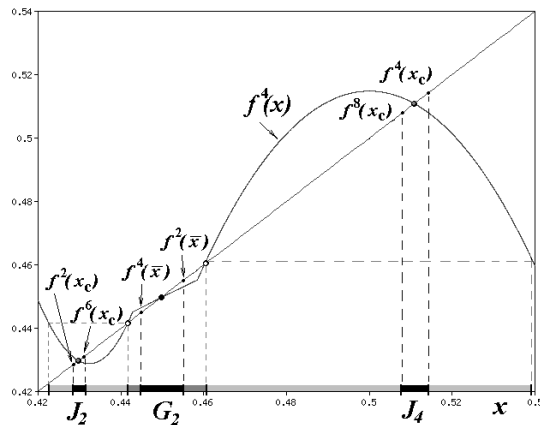


FIGURE 6. The enlarged window of Fig.5. Black circle indicates a point of the attracting cycle $\gamma_{0,2}$, gray circles indicate points of the attracting cycle $\gamma_{1,3}$ and white circles are points of repelling cycle $\gamma'_{1,3}$.

Figs 5 and 6 present an example of the map (1) for which two disjoint sets of cyclic absorbing intervals J_4 and G_2 exist: Fig.5 shows $f(x)$ and $f^4(x)$ for $a = 3.41$, $r = 1.9$, and Fig.6 is the enlarged window of Fig.5 with intervals J_2 , J_4 , G_2 and some points of the coexisting attracting 4-cycle $\gamma_{1,3}$ and attracting 2-cycle $\gamma_{0,2}$ of the map f . Note that their immediate basins of attraction, shown in Fig.6 by light gray and dark gray, respectively, are separated by the repelling 4-cycle denoted $\gamma'_{1,3}$ and its first preimage, born due to a fold bifurcation together with the attracting 4-cycle $\gamma_{1,3}$. Here and below $\gamma_{i,j}$ denotes any attracting cycle of period $i + j$ (not only a superstable one).

To see which regions in the (r, a) -parameter plane correspond to bistability let us return to Fig.3 and consider in detail two bistability regions: The first one denoted B_1 is related to the coexisting cycles $\gamma_{0,3}$ and $\gamma_{1,5}$, and the second one denoted B_2 corresponds to coexisting $\gamma_{0,6}$ and $\gamma_{1,5}$.

In the region B_1 the break point \bar{x} is attracted to the cycles $\gamma_{0,3}$, while the critical point x_c is attracted to the cycle $\gamma_{1,5}$. In the region B_2 \bar{x} is attracted to $\gamma_{0,6}$, and x_c is attracted to $\gamma_{1,5}$. The attracting 6-cycle $\gamma_{1,5}$ is born due to a fold bifurcation together with a repelling 6-cycle $\gamma'_{1,5}$. The curve corresponding to this fold bifurcation is shown by dashed line in Fig.3. It can be seen that the boundaries of the region B_1 are curves corresponding to the fold bifurcation of $\gamma_{1,5}$, and to the period-doubling and border-collision bifurcations of $\gamma_{0,3}$. The boundaries of B_2 are curves corresponding to the period-doubling bifurcation of $\gamma_{0,3}$, the BCB of $\gamma_{0,6}$ and the fold bifurcation of $\gamma_{1,5}$.

To illustrate the bistability and the bifurcations related to the cross-section of different boundaries of B_1 and B_2 , we present two 1D bifurcation diagrams (see Fig.3 in which the corresponding parameter values are indicated by two vertical straight lines with arrows). In Fig.7 one of the three branches of the 1D diagram is shown for $r = 3.268$ and $a \in [3.8404, 3.841]$.

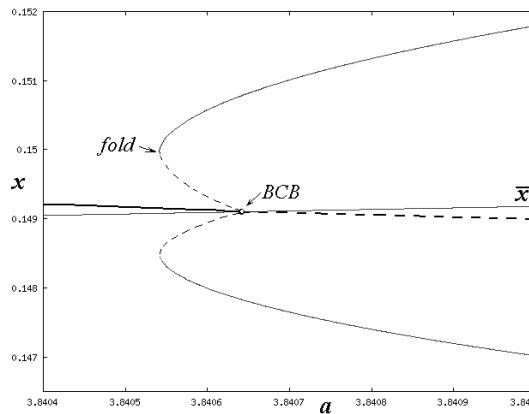


FIGURE 7. One of the three branches of the 1D bifurcation diagram of the map f at $r = 3.268$ and $a \in [3.8404, 3.841]$.

Increasing a in the indicated range the parameter point crosses the region B_1 : There is at first only the attracting cycle $\gamma_{0,3}$, then the fold bifurcation gives rise to the cycles $\gamma_{1,5}$ and $\gamma'_{1,5}$ (and, thus, to the bistability). Then the BCB occurs for a point of $\gamma_{0,3}$ and for two points of $\gamma'_{1,5}$ at the same time, resulting in the repelling cycle $\gamma'_{1,2}$. After the bifurcation the only attractor of the map is the cycle $\gamma_{1,5}$. The parameter values used in Fig.1 belong to the region B_1 . The repelling cycle $\gamma'_{1,5}$ and all its preimages of any rank are the separator of the two basins of attraction, say $\mathcal{B}(\gamma_{0,3})$ and $\mathcal{B}(\gamma_{1,5})$. Clearly, besides the two attracting cycles there exist infinitely many repelling cycles in I , constituting a chaotic repeller, thus the basins $\mathcal{B}(\gamma_{0,3})$ and $\mathcal{B}(\gamma_{1,5})$ have a fractal structure in I . It is also clear that two disjoint cyclical absorbing intervals \mathbf{J}_3 and \mathbf{G}_6 , bounded, respectively, by the images

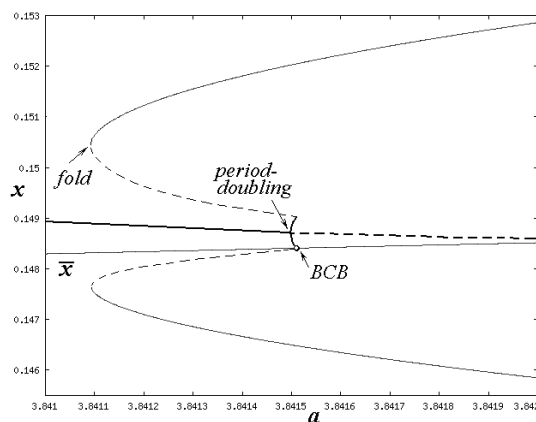


FIGURE 8. One of the three branches of the 1D bifurcation diagram of the map f at $r = 3.2714$, $a \in [3.841, 3.842]$.

of \bar{x} and x_c exist. The sets \mathbf{J}_3 and \mathbf{G}_6 belong to the immediate basins of $\gamma_{0,3}$ and $\gamma_{1,5}$, respectively, included in $\mathcal{B}(\gamma_{0,3})$ and $\mathcal{B}(\gamma_{1,5})$.

In Fig.8 one of the three branches of the 1D diagram is shown for $r = 3.2714$, $a \in [3.841, 3.842]$. Increasing a in the indicated range the parameter point crosses both the regions B_1 and B_2 : We see at first the cycle $\gamma_{0,3}$, then the fold bifurcation occurs resulting in the cycles $\gamma_{1,5}$ and $\gamma'_{1,5}$ (and bistability, entering B_1), then period doubling bifurcation of $\gamma_{0,3}$ gives rise to the cycle $\gamma_{0,6}$ (entering B_2) and, finally, the BCB occurs for a point of $\gamma_{0,6}$ and a point $\gamma'_{1,5}$ resulting in disappearance of these cycles, so that after the bifurcation the only attractor is the cycle $\gamma_{1,5}$.

Indeed, there are infinitely many bistability regions of such a kind as the regions B_1 and B_2 described above, which we call of 1st kind, in each “ m -box”, $m \geq 3$, (some of them are indicated by circles in Fig.3). Briefly, a bistability of 1st kind is related to the coexistence of attracting cycles of period $2^{i-1}m$ and $2^i m$, $i \geq 1$, or two attracting cycles of the same period $2^i m$.

But there are also infinitely many more complicated cases called bistability regions of 2nd kind related to the coexistence of an attracting cycle with an attracting cycle of other period, or with cyclic chaotic intervals. As an example of such a region, we present in Fig.9 the enlarged window III of Fig.2 where the largest of the shaded regions corresponds to coexistence of the attracting cycle $\gamma_{0,2}$ with the attracting cycle $\gamma_{1,3}$, or with cycles related to the period-doubling cascade of this cycle, or with other attractors following the logistic bifurcation scenario including coexistence with cyclic chaotic intervals. The other shaded region in Fig.9 is related to a similar kind of bistability but for the cycle $\gamma_{0,4}$. In the figure the dashed line corresponds to the fold bifurcation giving rise to the attracting and repelling cycles $\gamma_{1,3}$ and $\gamma'_{1,3}$. Thick line corresponds to the period-doubling bifurcation of $\gamma_{0,2}$, and thin lines are the BCB curves.

To illustrate the bistability of 2nd kind we present in Fig.10 one of the two branches of the 1D bifurcation diagram for the parameter values $r = 1.9312$, $a \in [3.4, 3.46]$ indicated in Fig.9 by the vertical straight line with an arrow. Increasing a in the indicated range we see that the attracting cycle $\gamma_{0,2}$ (thick line)

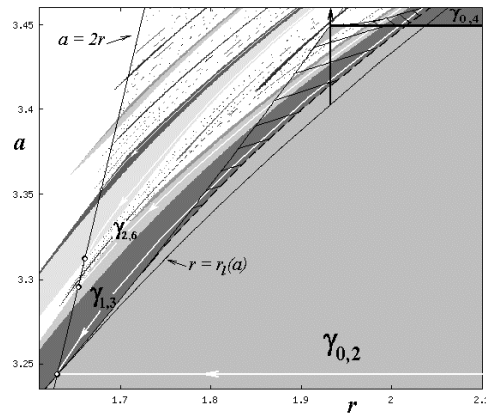


FIGURE 9. The enlarged window III of the 2D bifurcation diagram of the map f shown in Fig.2. Shaded regions correspond to bistability of the 2^{nd} kind.

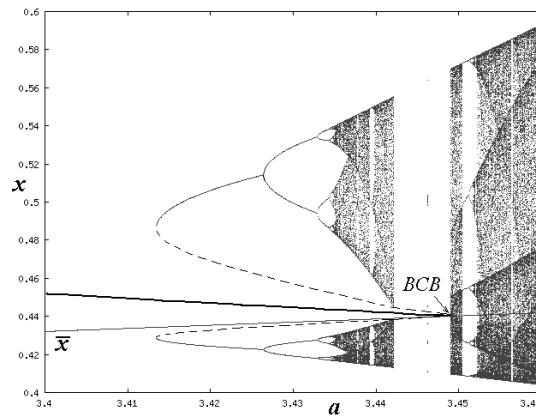


FIGURE 10. One of the two branches of the 1D bifurcation diagram of the map f at $r = 1.9312$, $a \in [3.4, 3.46]$.

coexists at first with the attracting cycle $\gamma_{1,3}$ (thin lines) born due to the fold bifurcation together with the repelling cycle $\gamma'_{1,3}$ (dashed lines), and then $\gamma_{0,2}$ coexists, consecutively, with all the cycles related to the period-doubling cascade of $\gamma_{1,3}$, and after with all other attractors, following the logistic bifurcation scenario. One can see also that the first homoclinic bifurcation for $\gamma'_{1,3}$ gives rise to a boundary crises for 4-cyclic chaotic interval, and surviving chaotic repeller reveals itself after the BCB of $\gamma_{0,2}$ occurring simultaneously with the BCB of $\gamma'_{1,3}$.

One more example of the 2nd kind bistability is indicated in Fig.4 as a shaded region in which the cycle $\gamma_{1,2}$ coexists either with $\gamma_{3,3}$, born due to the fold bifurcation (thin dashed line), or with the cycles related to the period-doubling cascade of $\gamma_{3,3}$, or with other attractors following the logistic bifurcation scenario.

5. Concluding remarks. In the present paper we have discussed the structure of the 2D bifurcation diagram of the unimodal piecewise smooth map f given in (1), in the case $x_c \geq \bar{x}$. Particular attention has been paid to the border-collision bifurcation of the superstable n -cycle of the map f , as well as to the bistability regions in the (r, a) -parameter plane. To end our considerations we add the following conjecture: Varying the parameter values in the region D_b one can observe three types of the BCB of an attracting cycle: 1) the attracting cycle becomes repelling while an attracting cycle of double period appears; 2) the attracting cycle merges with a repelling cycle of double period, and becomes repelling (see, for example, Fig.7); 3) the attracting cycle merges with a repelling cycle of the same period and they disappear (see Fig.8). The BCB of an attracting cycle to a cyclic chaotic interval can occur for $(r, a) \in D_r$, as well as other types of BCB. We leave the detailed investigation of the bifurcation structure of the region D_r as a subject for a future work.

REFERENCES

- [1] S. Banerjee, M.S. Karthik, G. Yuan and J.A. Yorke, *Bifurcations in One-Dimensional Piecewise Smooth Maps - Theory and Applications in Switching Circuits*, IEEE Trans. Circuits Syst.-I: Fund. Theory Appl., **47** (2000), no. 3, 389-394.
- [2] S. Banerjee, P. Ranjan and C. Grebogi, *Bifurcations in Two-Dimensional Piecewise Smooth Maps - Theory and Applications in Switching Circuits*, IEEE Trans. Circuits Syst.-I: Fund. Theory Appl., **47** (2000), no. 5, 633-642.
- [3] P. Collet and J.P. Eckmann, "Iterated Maps of the Interval as Dynamical Systems", Birkhauser, Boston, 1980.
- [4] M. Di Bernardo, M.I. Feigen, S.J. Hogan and M.E. Homer, *Local analysis of C-bifurcations in n-dimensional piecewise smooth dynamical systems*, Chaos, Solitons & Fractals, **10** (1999), no. 11, 1881-1908.
- [5] R. Day, *Irregular growth cycles*, The American Economic Review, **72** (1982), no. 3, 406-414.
- [6] R. Day, "Complex Economic Dynamics", MIT Press, Cambridge, 1994.
- [7] R. Day and G. Pianigiani, *Statistical dynamics and economics*, J. of Economic Behavior and Organization, **16** (1991), 37-84.
- [8] W. De Melo and S. van Strien, "One-Dimensional Dynamics", Springer, New York, 1993.
- [9] R.L. Devaney, "An Introduction To Chaotic Dynamical Systems", The Benjamin/Cummings Publ. Co. Inc., Menlo Park, 1986.
- [10] J. Graczyk and G. Swiatek, *Smooth unimodal maps in the 1990s*, Ergodic Theory Dynam. Systems, **19** (1999), 263-287.
- [11] C. Halse, M. Homer and M. di Bernardo, *C-bifurcations and period-adding in one-dimensional piecewise-smooth maps*, Chaos, Solitons & Fractals, **18** (2003), 953-976.
- [12] B.L. Hao, "Elementary Symbolic Dynamics and Chaos in Dissipative Systems", World Scientific, Singapore, 1989.
- [13] C.H. Hommes and H. Nusse, *Period three to period two bifurcations for piecewise linear models*, Journal of Economics, **54** (1991), no. 2, 157-169.
- [14] M. Jakobson, *Absolutely continuous invariant measures for one-parameter families of one-dimensional maps*, Comm. Math. Phys., **81** (1981), 39-88.
- [15] M. Lyubich, *Regular and stochastic dynamics in the real quadratic family*, Proc. Nat. Acad. Sci. USA, **95** (1998), 14025-14027 (electronic).
- [16] V.L. Maistrenko, Yu.L. Maistrenko and I. Sushko, *Attractors of piecewise linear maps of straight line and plane*, Prepr. Acad. of Sci. of Ukraine, Institute of Mathematics: 92.33 (1992), 1-55 (in Russian).

- [17] Yu.L. Maistrenko, V.L. Maistrenko and L.O. Chua, *Cycles of chaotic intervals in a time-delayed Chua's circuit*, International Journal of Bifurcation and Chaos, **3** (1993), no. 6, 1557-1572.
- [18] Yu.L. Maistrenko, V.L. Maistrenko and S.I. Vikul, *On period-adding sequences of attracting cycles in piecewise linear maps*, Chaos, Solitons & Fractals **9** (1998), no. 1, 67-75.
- [19] N. Metropolis, M.L. Stein and P.R. Stein, *On finite limit sets for transformations on the unit interval*, J. Comb. Theory, **15** (1973), 25-44.
- [20] C. Mira, "Chaotic Dynamics", World Scientific, Singapore, 1987.
- [21] H.E. Nusse and J.A. Yorke, *Border-collision bifurcations including period two to period three for piecewise smooth systems*, Physica D, **57** (1992), 39-57.
- [22] H.E. Nusse and J.A. Yorke, *Border-collision bifurcations for piecewise smooth one-dimensional maps*, International Journal of Bifurcation and Chaos, **5** (1995), no. 1, 189-207.
- [23] T. Puu and I. Sushko Ed.s, "Oligopoly and Complex Dynamics: Tools and Models", Springer, New York, 2002.
- [24] I. Sushko, T. Puu and L. Gardini, *The Hicksian floor-roof model for two regions linked by interregional trade*, Chaos Solitons & Fractals, **18** (2003), 593-612.
- [25] A.N. Sharkovsky, S.F. Kolyada, A.G. Sivak and V.V. Fedorenko, "Dynamics of One-dimensional Maps", Kluwer Academic Publ., Boston, 1997.
- [26] D. Singer, *Stable orbits and bifurcations of maps of the interval*, SIAM J. Appl. Math., **35** (1978), 260-267.
- [27] Z.T. Zhusubaliyev and E. Mosekilde, "Bifurcations and Chaos in Piecewise - Smooth Dynamical Systems", World Scientific, Singapore, 2003.

Received April, 2004; revised February 2005.

E-mail address: sushko@imath.kiev.ua

E-mail address: anna.agliari@unicatt.it

E-mail address: gardini@econ.uniurb.it